Cancer Cell International

RESEARCH Open Access

Esketamine reduces postoperative depression in breast cancer through TREK-1 channel inhibition and neurotransmitter modulation

Jiachi Xu[1], Mingcan Li[2], Yu Hu[3], Qin Yang[4], Qiang Long[3] and Hui Zhou[1*]

Abstract

Postoperative depression significantly affects the quality of life of breast cancer patients. This study explores the potential therapeutic effects of esketamine on postoperative depression through modulation of the TREK-1 two-pore domain potassium channel. We analyzed data from 54 female breast cancer patients who underwent surgery at our hospital between 2019 and 2023, dividing them into experimental and control groups based on esketamine treatment. Transcriptomic sequencing of hippocampal neurons from rats identified potassium ion-related pathways and key regulatory genes, including TREK-1, influenced by esketamine. In vitro studies showed that esketamine primarily alleviates depressive symptoms by inhibiting TREK-1 protein expression, enhancing GABA neurotransmitter release, and improving neuronal activity, while overexpression of TREK-1 reversed these effects. Esketamine's inhibition of TREK-1 channels and promotion of hippocampal neuron activity effectively alleviate postoperative depression in breast cancer patients, suggesting a novel therapeutic strategy.

Keywords Postoperative depression, Breast cancer, Esketamine, TREK-1 channels, Hippocampal neurons

Introduction

Breast cancer, as one of the most common types of cancer in women globally, has led to significant post-treatment consequences, particularly depression, becoming a crucial factor affecting patients' quality of life [1, 2]. Studies have shown that female breast cancer patients often experience varying degrees of mental health issues post-surgery, with depression symptoms being particularly prevalent [3–5]. This emotional disturbance not only impacts the patients' psychological well-being but also affects their biological recovery and quality of life [6–8]. Currently, the treatment of postoperative depression in breast cancer presents numerous challenges, as traditional antidepressant medications often require a lengthy period to take effect and come with various side effects [9–11]. Therefore, developing more effective treatment strategies is an urgent clinical need. In this context, this study aims to explore new pharmacological treatment approaches to enhance treatment efficiency and alleviate patient suffering.

Depression is a complex mood disorder involving multiple biological pathways and neurochemical changes [12–14]. The hippocampus, a region in the brain closely associated with emotion regulation and memory

*Correspondence:
Hui Zhou
zhouhui.17@csu.edu.cn
[1] Department of General Surgery, Second Xiangya Hospital, Central South University, No. 139, Renmin Middle Road, Furong District, Changsha, Hunan, China
[2] The First Affiliated Hospital of University of South China, Hengyang, Hunan, China
[3] First Clinical Medical College, Shanxi Medical University, Taiyuan, China
[4] University of South China, Hengyang, Hunan, China

formation, plays a central role in the development of depression [15, 16]. Studies indicate that depressed patients often exhibit reduced hippocampal volume and weakened neuroplasticity, which is related to neuronal dysfunction caused by chronic stress [17]. Furthermore, the imbalance of neurotransmitters such as serotonin, norepinephrine, and dopamine is considered a key factor in the onset of depression [18, 19]. However, the effectiveness of traditional antidepressant therapy is often limited due to the unique physiological and psychological conditions following breast cancer surgery [20, 21].

In recent years, esketamine, as an NMDA receptor antagonist, has demonstrated significant potential in rapid antidepressant therapy [22]. Unlike traditional antidepressant medications, esketamine can swiftly enhance patients' mood states. Its unique mechanism of action includes rapidly enhancing neuroplasticity, improving interneuronal signaling, and directly influencing the neurotransmitter system [23–25]. This rapid antidepressant effect provides a new treatment option for clinical scenarios requiring immediate intervention, such as postoperative depression in breast cancer [26, 27]. Although the specific antidepressant mechanisms of esketamine are not fully understood, its demonstrated efficacy and good tolerability in clinical trials have made it a hot research topic [28, 29].

TREK-1 is a background potassium ion channel widely distributed in the human brain, particularly in regions involved in regulating emotion and pain perception [30, 31]. By modulating potassium ion flow, TREK-1 influences the excitability of nerve cells, thereby impacting neural transmission. Changes in TREK-1 expression are closely associated with emotional regulation imbalance in depressive states [32, 33]. Studies have demonstrated that the inhibition of TREK-1 significantly affects depressive symptoms, suggesting its potential as a target for antidepressant therapy [34, 35]. In light of this, our research delves into the regulatory effects of esketamine on the TREK-1 channel and how this modulation affects the amelioration of symptoms related to postoperative depression in breast cancer.

This study aims to explore the molecular mechanisms by which esketamine regulates TREK-1 two-pore domain potassium channels in postoperative depression in breast cancer. Through clinical and biological experiments on patients with postoperative depression in breast cancer and animal models, we seek to validate the effects of esketamine on TREK-1 and its antidepressant properties. We hypothesize that esketamine, by inhibiting the TREK-1 channel, can enhance neuronal activity, thus effectively improving depressive symptoms. This finding not only offers new strategies for the treatment of postoperative depression in breast cancer but also potentially sheds light on broader treatments for depression. Furthermore, this study aims to deepen our understanding of the complex pathophysiological mechanisms of depression, thereby fostering innovation and development in relevant therapeutic approaches.

Materials and methods

Patient data collection

This randomized, double-blind, controlled trial enrolled a total of 54 breast cancer patients who underwent modified radical mastectomy between March 2019 and March 2023. Patient demographics, including age, weight, height, and pathological type, were collected (Table S1). The pathological types of all patients were uniformly confirmed by the hospital's pathology department to ensure data accuracy. Detailed treatment histories for each patient, such as the type of surgery, chemotherapy, and radiation therapy, were meticulously recorded to ensure data integrity. The treatment histories of all patients were provided by the attending physicians and cross-checked by members of the research team. Patients were consecutively recruited during the study period and randomly assigned to different groups based on whether they received esketamine treatment. Esketamine injections (purchased from Jiangsu Hengrui Pharmaceutical Co., Ltd., Product Code: KH080601) were subcutaneously administered twice a week at 0.5 mg/kg to the abdominal wall for four weeks with a minimum interval of 3 days between treatments, while the control group consisted of patients not receiving drug therapy [36]. Additionally, these patients were diagnosed using imaging and histological methods. Prior to surgery, all patients underwent evaluation using the Hamilton Depression Scale (HAMD-17), with scores categorized as 0–7 indicating no depression, 8–16 mild depression, 17–23 moderate depression, and ≥24 severe depression. Only those patients with HAMD-17 scores between 8 and 23, indicative of mild to moderate depression, were included in the study [37]. The age range of all patients was between 18 and 65 years, with an American Society of Anesthesiologists (ASA) physical status classification of I-II. Patients with a preoperative HAMD-17 score of 24 or 7, those with other psychiatric illnesses (such as schizophrenia and bipolar disorder), a history of psychiatric disorders before the study, prior use of psychiatric medication, or other severe systemic conditions (including severe cardiac, renal, or hepatic diseases) were excluded from the study.

Due to studies suggesting that immediate breast reconstruction may increase surgical complications and failure rates, it was not recommended for these patients to undergo immediate breast reconstruction [38]. All

patients provided informed consent. This study was approved by the hospital's ethics committee.

Construction of animal models

Forty female Wistar rats (strain 619, Charles River, Germany) were selected for the study. The animals were individually housed, with ad libitum access to food and water, and maintained under constant temperature (22 ± 2 °C) and humidity (50 ± 5%) with a 12-h light/dark cycle. All procedures followed the rules and principles of Directive 86/609/EEC and were approved by the local bioethics committee. Every effort was made to minimize animal suffering and reduce the number of animals used.

The control group of rats remained undisturbed in their cages and housed separately throughout the entire process. The experimental group of rats, however, were individually housed and subjected to the following stressors: (a) 12 h of water deprivation; (b) 12 h of food deprivation; (c) 12 h of constant illumination; (d) 3 h of cage switching; (e) 12 h of soiled bedding (200 ml water with 100 g sawdust bedding); (f) 30 min of predator sounds (cat); (g) 24 h of reversed light–dark cycle; (h) 15 h of paired housing; (i) swimming in cold water (4 °C, 5 min); (j) swimming in hot water (40 °C, 5 min); (k) tail pinching for 2 min (2 cm from the base of the tail); (l) 2 h of restraint stress; (m) electrical stimulation (3 min). Three different stressors were applied to the rats each day for 4 weeks in a chronic and unpredictable manner [39].

Using the known TREK-1 sequence in NCBI, Shanghai Hanheng Biotechnology Co., Ltd. (Shanghai, China) was commissioned to construct oe-NC and oe-TREK-1 lentiviral vectors in the lentiviral vector pHBLV-CMV-MCS-EF1-Puromycin. After one week of acclimation to the housing environment, each rat received a tail vein injection of lentivirus at a dose of 5×10^6 TU (Transduction Units), and subsequent procedures were conducted 48 h later [40].

The esketamine injection was purchased from Jiangsu Hengrui Pharmaceutical Co., Ltd., China (Product Code: KH080601). After 4 weeks of Chronic Unpredictable Mild Stress (CUMS) stimulation, rats were intraperitoneally injected daily with either the vehicle (saline solution) or esketamine (10 mg/kg). The drug treatment lasted for a total of 3 weeks, followed by an additional week of CUMS during the drug withdrawal period [41].

Based on the above protocol, the rats were divided into the following groups: (1) sham group (normal rats without undergoing CUMS procedure) ($n = 8$); (2) CUMS group (depressive rat model subjected to CUMS procedure) ($n = 8$); (3) CUMS + esketamine group (depressive rat model subjected to CUMS procedure receiving esketamine treatment) ($n = 8$). The (4) CUMS + esketamine + oe NC and (5) CUMS + esketamine + oe TREK-1 groups underwent the CUMS + esketamine treatment after the construction of the rat models by injecting oe NC and oe TREK-1 lentivirus, respectively.

High throughput sequencing and analysis of cellular response to esketamine treatment

Three hippocampal neuron samples from a control group (CUMS) of rats and three hippocampal neuron samples from a group treated with esketamine (CUMS + esketamine) were randomly selected. Total RNA was extracted from the six cell samples using an RNA isolation reagent (12183555, Invitrogen, USA) and quantified by measuring the OD values of total RNA with a UV–Visible spectrophotometer (BioSpectrometer Basic, Eppendorf, USA). The integrity of the total RNA was assessed using agarose gel electrophoresis. High-quality total RNA was reverse transcribed into cDNA, and RNA libraries were constructed. Sequencing was performed using Illumina's NextSeq 500 platform, with raw image data converted to raw reads through base calling. To ensure the quality of the raw reads, cutadapt was utilized to remove sequencing adapter sequences and filter out low-quality sequences, leaving behind the "clean reads." These clean reads were then aligned to the rat reference genome using Hisat2 software, and gene expression was quantified using the R software package, resulting in a gene expression matrix [42].

Screening of differentially expressed genes

The "limma" package in R language was utilized to filter DEGs from high throughput sequencing data, where genes with $|\log2FC| > 1$ & p-value < 0.05 were considered as the screening criteria. A volcano plot was generated using the ggplot2 R package, and a heat map was constructed using the pheatmap R package. The DEGs in the samples were subjected to Gene Ontology (GO) and Kyoto Encyclopedia of Genes and Genomes (KEGG) pathway enrichment analysis through the Xiantao Academic database (https://www.xiantaozi.com/) [43–45].

Machine learning for identifying key gene sets

Three machine learning methods—Least Absolute Shrinkage and Selection Operator (LASSO), Support Vector Machine (SVM), and Random Forest (RF)—were utilized to identify essential gene sets associated with the treatment of depression using esketamine. The LASSO regression analysis was conducted using the glmnet package (version 4.0-2) in R language. SVM analysis was performed with the e1071 package (version 1.7-3), while RF analysis utilized the randomForest package (version 4.6-14). The dataset was divided into training and testing sets in a 70:30 ratio [46, 47].

Extraction and cultivation of hippocampal neurons

Brain membranes were extracted from Wistar rats (619, Charles River, Germany), and the hippocampi were treated with trypsin (0.027%, T2600000, Sigma) in a culture chamber at 35 °C, under 95% O_2 and 5% CO_2, for 40 min. The trypsin solution was then removed, and the hippocampi were washed multiple times with N2-hydroxyethylpiperazine-N′-2-ethanesulfonic acid (HEPES) buffer solution (60117ES60, Yisheng Biotech (Shanghai) Co., Ltd.), devoid of Ca^{2+} and Mg^{2+}. Subsequently, the hippocampi were placed in a warm growth medium (DMEM) supplemented with 25 mM HEPES, 10% fetal bovine serum (12483020, Gibco), 10% Hams F-12 (11765047, Gibco), and 50 µl/ml penicillin–streptomycin (15140148, Gibco). The culture medium was changed thrice weekly. After 7–10 days in vitro cultivation, non-neuronal cell growth was inhibited for 48 h using cytosine arabinoside (5 µM, C1768, MCE). The neurons were utilized for subsequent experiments after 3–4 weeks of in vitro culture, and their purity was confirmed by immunofluorescence staining for the neuronal cell marker MAP2 and the glial cell marker GFAP [48].

To simulate depression in vitro, hippocampal neuron cells were pre-treated with 300 µM NMDA (N-methyl-D-aspartic acid, HY-17551, MCE) for 24 h, followed by the introduction of 100 µg/ml esketamine [49] to the treated cells. Based on the known TREK-1 sequence in NCBI, Shanghai Hanheng Biotechnology Co., Ltd. (Shanghai, China) was commissioned to construct oe-NC and oe-TREK-1 into the lentivirus vector pHBLV-CMV-MCS-EF1-Puromycin. After 24 h of incubation in a culture chamber, these treated hippocampal neuron cells were infected with the lentivirus. Following viral infection for 72 h, the culture medium was replaced with a medium containing 4 µg/mL puromycin (Invitrogen, A1113803), and the cells were cultured for at least 14 days. Puromycin-resistant cells were expanded for 9 days in a medium containing 2 µg/mL puromycin (Invitrogen, A1113803), then transferred to a puromycin-free medium to establish stable overexpression of TREK-1 in hippocampal neuron cells. The efficiency of TREK-1 overexpression was verified through Western blot analysis [50].

Esketamine, purchased from Jiangsu Hengrui Pharmaceutical Co., Ltd., China (catalog number KH080601), was dissolved in DMSO. The cells were treated with 100 µg/ml esketamine for 24 h [51].

Based on the aforementioned treatment, the cells were categorized into the following groups: (1) control group (hippocampal neuron cells isolated from rats); (2) CUMS group (neuronal cells treated with NMDA); (3) CUMS + esketamine group (neuronal cells in the CUMS group treated with esketamine); (4) CUMS + esketamine + oe-TREK-1 group (neuronal cells in the CUMS group infected with oe-TREK-1 lentivirus then treated with esketamine); (5) CUMS + esketamine + oe-NC group (neuronal cells in the CUMS group infected with oe-NC lentivirus then treated with esketamine).

Whole-cell patch-clamp techniques

Whole-cell patch-clamp techniques were performed using borosilicate glass capillary electrodes (BS4 30-0054, Harvard Apparatus, Holliston, MA, USA) with an outer diameter of 1.5 mm and an inner diameter of 0.80 mm. The resistance of the pipette when filled with an internal solution was maintained between 8 and 12 MΩ. The pipette holder was mounted on a CV203BU head stage (Molecular Devices, Sunnyvale, CA, USA), which was connected to a three-axis coarse manipulator and a micromanipulator (Narishige, Tokyo, Japan). Signal amplification and recording were conducted using an Axopatch 200B amplifier and pClamp 10.7 software (Molecular Devices, Sunnyvale, CA, USA). Data were filtered at 5 kHz and digitized at 10 kHz using a Digidata 1440A analog-to-digital converter (Molecular Devices, Sunnyvale, CA, USA). Voltage ramp protocol ranged from a holding potential of +10 to −90 mV, then ramped for 0.1 s to +110 mV before returning to +10 mV (repeated every 10 s). Liquid junction potential (+10 mV) between the pipette and bath solution was corrected during data analysis. The pipette was filled with an internal solution containing 30 mM CsCl (289329, Sigma-Aldrich), 2 mM $MgCl_2$ (M1028, Sigma-Aldrich), 110 mM L-aspartic acid (1.00129, Sigma-Aldrich), 1 mM EGTA (E0396, Sigma-Aldrich), 10 mM HEPES (60117ES60, Yisheng Biotech (Shanghai) Co., Ltd.), 4 mM ATP (11140965001, Sigma-Aldrich), 0.1 mM GTP (10106399001, Sigma-Aldrich). The use of L-aspartic acid in the internal pipette solution precluded chloride ion currents from contributing to the evaluation of TRPM3. Cells displaying unstable currents were excluded from the analysis [52].

Detection of protein expression by western blot

Cells and tissues from different groups were collected and lysed on ice for 30 min in RIPA lysis buffer (P0013B, Biyuntian, Shanghai, China) containing 1% PMSF, followed by centrifugation at 14,000×*g* and 4 °C for 20 min to collect the supernatant. Protein concentrations in the extracts were determined using the BCA method (P0012S, Biyuntian, Shanghai, China). Samples were denatured by adding an appropriate amount of 5× loading buffer and boiling at 100 °C for 10 min, with a protein loading amount of 50 µg. Electrophoresis was performed using prepared separating and concentrating gels, and after electrophoresis, bands containing the target

proteins were transferred onto a PVDF membrane. The PVDF membrane was then blocked in 5% non-fat milk powder at room temperature for 1 h, followed by overnight incubation at 4 °C with the primary antibodies rabbit anti-TREK-1 (GTX16653, GeneTex, USA) and rabbit anti-GAPDH (ab8245, Abcam), with GAPDH serving as an internal control. After washing with phosphate-buffered saline with Tween (PBST) at room temperature, an HRP-conjugated goat anti-rabbit IgG secondary antibody (ab205718, Abcam, UK) was used. Signal detection was performed using the ECL detection system (32209, Thermo Fisher Scientific, USA), followed by exposure in an imaging system (Amersham Imager 600, USA) for visualization [53, 54]. Finally, grayscale analysis was conducted using Image J. The experiment was conducted in triplicate.

Cell proliferation experiment using CCK-8 assay

Cell proliferation was assessed using the Cell Counting Kit-8 (CCK-8) (Beyotime, C0037, Shanghai, China). Cells were seeded in a 96-well plate. At 0, 12, 24, 36, 48, 60, and 72 h, 10 μL of CCK-8 solution was added to each well. Subsequently, the cells were incubated for an additional 1–2 h. The absorbance of cells at 450 nm wavelength was measured [55]. Each group had 6 replicate wells, and the experiment was repeated 3 times.

Immunofluorescent staining

Isolated hippocampal neurons were fixed on glass slides using 4% formaldehyde (F1635, Sigma-Aldrich). Immunofluorescent staining was performed for the neuronal cell marker MAP2 and the glial cell marker GFAP. Specific antibodies targeting MAP2 (neuronal cell marker) (ab183830, Abcam, UK) and GFAP (glial cell marker) (ab7260, Abcam, UK) were utilized. Cells incubated with the MAP2 antibody were stained using secondary antibodies labeled with Alexa Fluor® 647 (ab314474, Abcam, UK), while those incubated with the GFAP antibody were stained using secondary antibodies labeled with Alexa Fluor® 488 (ab222914, Abcam, UK). Nuclear staining was achieved with DAPI (C1005, Beyotime). The specimens were imaged at 400 times magnification using an inverted Olympus FV1000 laser scanning confocal microscope (Olympus). Fluorescence intensity measurements were conducted using ImageJ software to analyze the percentage of positively stained cells in randomly selected areas [56].

Flow cytometry analysis of cell apoptosis

Apoptosis analysis of hippocampal neurons was performed using the Annexin V-FITC/PI apoptosis detection kit (CA1020, Cell Signaling Technology) following the manufacturer's instructions. The treated cells were collected and resuspended in a binding buffer, then incubated with Annexin V-FITC and PI dyes for 15 min in the dark at room temperature. Flow cytometry analysis was carried out using a flow cytometer (BD Biosciences, USA), and the apoptosis percentage was calculated using analysis software [57].

ELISA detection of neurotransmitter levels

An appropriate amount of cell culture supernatant was used to determine the neurotransmitter levels in cells following the manufacturer's instructions using the rat ELISA kit for GABA provided by Abcam (ab287793, Abcam). The ELISA assay was performed according to the kit instructions, and the OD values were read using a microplate reader (BioTek, USA) to calculate the concentration of GABA protein in the samples [58, 59].

Behavioral testing

Sucrose Preference Test (SPT): The SPT was conducted before and after CUMS induction. All rats were individually housed and deprived of water and food for 8 h prior to the test. During the experiment, rats were given free access to two bottles containing either a 1% sucrose solution or tap water for 15 h. To avoid potential side preference effects, the positions of the bottles were switched midway through the test.

Open Field Test (OFT): On day 56, an OFT was conducted using a computer-assisted control system developed by Wang et al. (2010) to measure the animals' locomotor activity. The apparatus consisted of four metal boxes (30 cm in diameter, 40 cm in height, accommodating four rats simultaneously), each equipped with a camera fixed on top to allow observation. The rats were placed in the center of each metal box for 3 min of free exploration, followed by a 10-min test of locomotor activity.

Forced Swim Test (FST): The FST was conducted on the day following the OFT. Rats were individually placed in a plastic cylinder filled with water (25 °C) to a depth of 15 cm and forced to swim for 6 min. The software (forceswim video analysis system 2.0) was used to record and calculate the immobility during the final 4 min of the test [39].

Nissl staining

Brain cortical tissues surrounding the injury were fixed in formaldehyde, dehydrated, embedded in paraffin, and sectioned into 4 μm slices in groups of five. Following rehydration in gradient concentrations of alcohol, Nissl staining was performed using a commercial kit (GS0275, Beijing Baiolibo Technology Co., Ltd., Beijing, China). Images were captured using a Nikon microscope Ts2R

(Tokyo, Japan), and structural abnormalities of neurons were quantified using Image J software [51].

TUNEL staining

TUNEL staining for apoptotic cells was conducted using a one-step TUNEL assay kit (C1086, Beyotime, Shanghai, China). Initially, the sections were treated with 0.1% Triton X-100 (ST795, Beyotime, Shanghai, China) at 4 °C for 3 min, incubated with proteinase K for 15 min, and then incubated with 50 μL of TUNEL reaction mixture. After 1 h of incubation at 37 °C in the dark, the plates were sealed with an anti-fade mounting solution, and fluorescence intensity was observed under a fluorescence microscope (DMI4000 B, Leica Microsystems, Germany). Five high-power fields were randomly selected to determine the number of TUNEL-positive cells [60].

Statistical analysis

The data were derived from at least three independent experiments, and the results are presented as mean ± standard deviation (Mean ± SD); for comparisons between two groups, two independent sample t-tests were employed; for comparisons involving three or more groups, a one-way analysis of variance (ANOVA) was conducted. If ANOVA indicated significant differences, Tukey's honestly significant difference (HSD) post hoc test was performed to compare differences between groups. In cases of non-normal distribution or unequal variances, the Mann–Whitney U test or Kruskal–Wallis H test was utilized. All statistical analyses were conducted using GraphPad Prism 9 (GraphPad Software, Inc.) and the R language. The significance level for all tests was set at 0.05, with a two-tailed p-value less than 0.05 considered statistically significant.

Results

Esketamine effectively alleviates depression symptoms in breast cancer patients

This study included a total of 54 female patients who underwent breast cancer surgery at our institution between 2019 and 2023. The patients' ages ranged from 30 to 70 years, with a mean age of 48.5 years. The pathology department of our institution confirmed the pathological types of all patients, with invasive ductal carcinoma being the most prevalent at 70% (Fig. 1A).

The Hamilton Depression Scale (HAMD-17) scores at 6 months post-surgery show that patients treated with esketamine had significantly lower scores across all levels of depression severity compared to the control group, indicating a marked improvement in depressive symptoms (Fig. 1B). At six months post-surgery, approximately 30% of patients exhibited mild to moderate depressive symptoms based on the Hamilton Depression Scale, with 5% of patients showing severe depressive symptoms (Fig. 1C). Patients were divided into an experimental group receiving esketamine ($N=27$) and a control group ($N=27$). The results of the Hamilton Depression Scale scores indicated that compared to the control group, patients in the esketamine group demonstrated significant symptom improvement, with a notable increase in the proportion of in the normal group and a significant decrease in the proportions of patients with mild to moderate and severe depression symptoms (Fig. 1D).

Esketamine improves depressive symptoms in a rat model

To further investigate the molecular mechanisms through which esketamine exerts its function, we constructed a rat model of depression using a 28-day CUMS protocol and assessed the success of the model through behavioral observations [39]. Results from the SPT indicated that compared to the Sham group, rats in the CUMS group showed a significant reduction in sucrose intake. Following treatment with esketamine (10 mg/kg), the CUMS rats in the CUMS + esketamine group exhibited a significant increase in sucrose consumption compared to the CUMS group (Fig. 2A). The FST results revealed that in comparison to the Sham group, rats in the CUMS group displayed a notable increase in immobility time. However, after treatment with esketamine (10 mg/kg), the CUMS rats in the CUMS + esketamine group showed a significant decrease in immobility time compared to the CUMS group (Fig. 2B). Additionally, results from the OFT demonstrated that compared to the Sham group, rats in the CUMS group exhibited a significant decrease in the number of crossings in the open field. Treatment with esketamine (10 mg/kg) resulted in a significant increase in the number of crossings in the CUMS + esketamine group compared to the CUMS group (Fig. 2C). Esketamine treatment in the CUMS rat model significantly alleviated depressive symptoms, with values in behavioral tests (SPT, FST, OFT) comparable to the normal control group, demonstrating the potential of esketamine to restore normal behavioral levels.

These findings suggest that the CUMS protocol successfully established a rat model of depression, and esketamine effectively alleviated depressive symptoms in the rat model.

Transcriptome sequencing reveals key gene TREK-1 impacted by esketamine in improving postoperative depression

Esketamine, after administration, undergoes rapid metabolism in the body, converting into active metabolites such as norketamine. These metabolites, particularly norketamine, are known to continue modulating neural pathways linked to depression. The transformation of

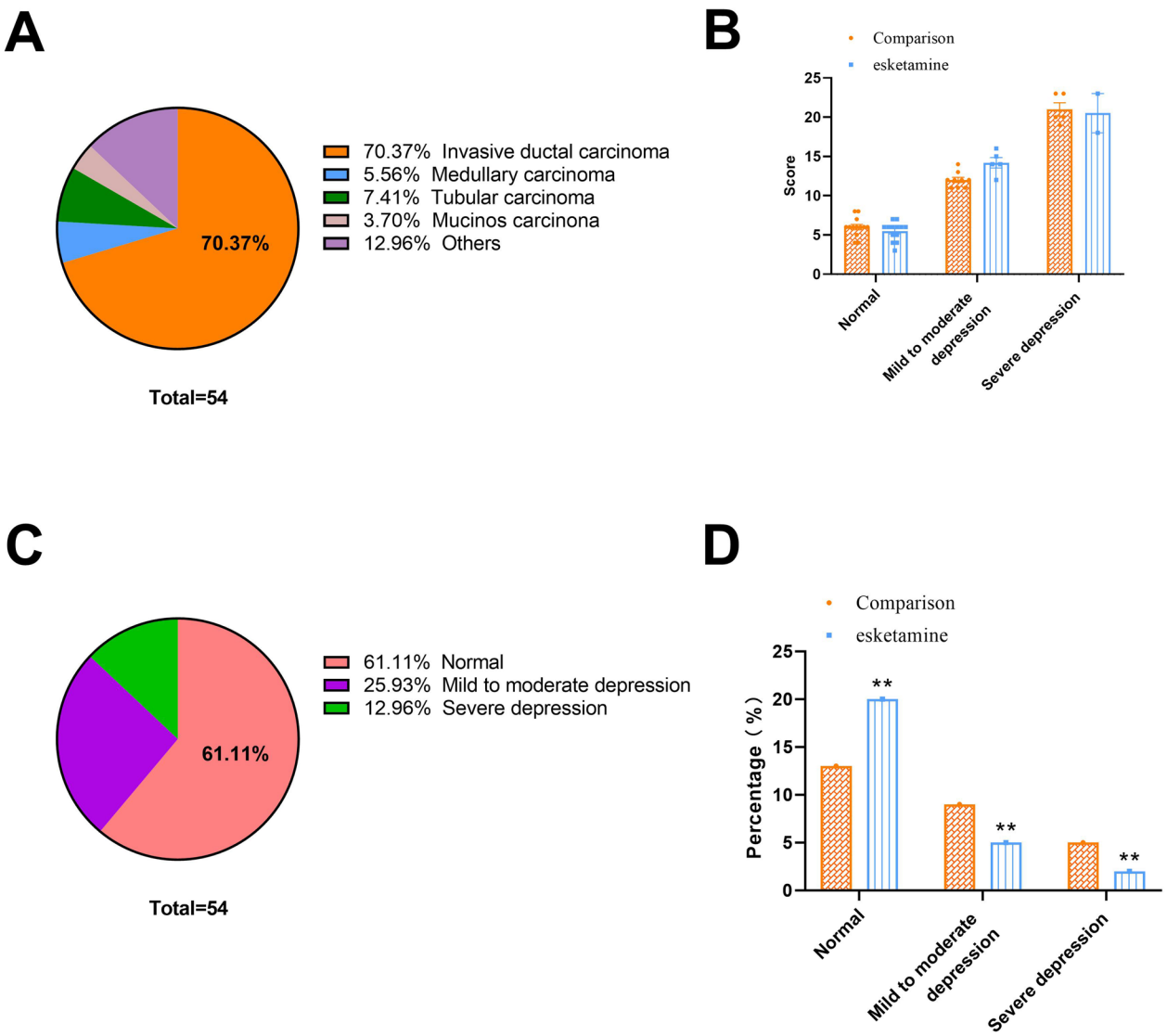

Fig. 1 Analysis of pathological types distribution, postoperative depression symptoms, and brain MRI Results in breast cancer patients. **A** Proportion of different pathological types of breast cancer in the study population ($n=54$); **B** The postoperative 6-month Hamilton Depression Rating Scale scores of patients treated with escitalopram ($n=54$) or in the control group ($n=54$); **C** Statistical analysis of Hamilton Depression Scale scores in patients at 6 months postoperatively ($n=54$); **D** Statistical analysis of Hamilton Depression Scale scores at 6 months postoperatively in patients treated with esketamine ($n=54$) or control ($n=54$). *$p<0.05$, **$p<0.01$

esketamine into these active compounds is crucial, as they further inhibit the TREK-1 channel and enhance the antidepressant effects.

Subsequently, we collected hippocampal neuron samples from three control group (CUMS) rats and three esketamine treatment group (CUMS + esketamine) rats for high throughput sequencing. Differential expression analysis revealed significant gene differences between the esketamine treatment group and the control group, identifying a total of approximately 9 DEGs, all of which were downregulated genes (Fig. 3A). The expression patterns of these 9 differential genes in the high throughput sequencing results are shown in Fig. 3B.

Following this, the identified DEGs underwent GO and KEGG functional enrichment analyses. The GO enrichment analysis results demonstrated that the differential genes were mainly enriched in biological processes such as fear response, behavioral defense response, and behavioral fear response; cellular components including neuron projection terminus, axon terminus, and ion channel complex; and molecular functions such as neurotransmitter receptor activity, acetylcholine receptor binding,

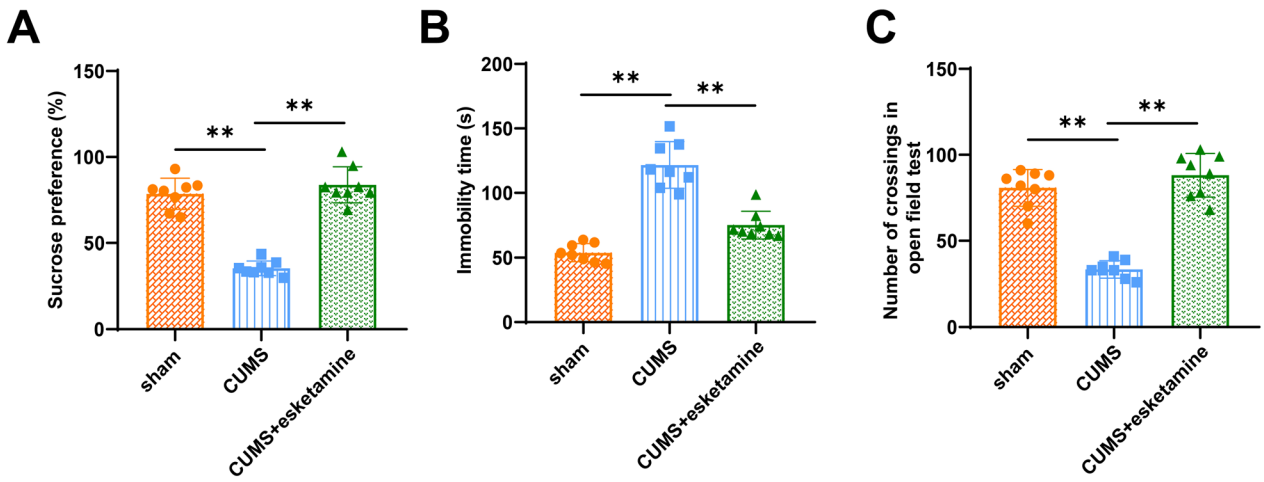

Fig. 2 Construction of depressive rat models and phenotypic evaluation after esketamine treatment. **A** CUMS depressive rat model, evaluation of sucrose intake in CUMS depressive rat model after esketamine treatment ($n=8$); **B** CUMS depressive rat model, statistical analysis of immobility time in CUMS depressive rat model after esketamine treatment ($n=8$); **C** CUMS depressive rat model, behavioral performance in OFT after esketamine treatment ($n=8$). *$p<0.05$; **$p<0.01$

and gated channel activity (Figure S1A). KEGG enrichment analysis results indicated that the differential genes were predominantly enriched in pathways like Neuroactive ligand–receptor interaction, Gap junction, and Gastric acid secretion (Figure S1B). This finding suggests that esketamine metabolites, particularly hydroxynorketamine (HNK) types such as (2R,6R)-HNK, may improve postoperative depression in breast cancer by modulating ion channels, including TREK-1, and altering neuronal system functionality.

In the end, we conducted a multivariate Cox analysis using the LASSO regression on these 9 differential genes (Fig. 3C, D), evaluated the gene importance using the random forest algorithm (Fig. 3E, F), and extracted relevant genes for improving postoperative depression by esketamine metabolites through the SVM-RFE analysis method (Fig. 3G). Ultimately, we successfully identified a key gene, KCNK2 (Fig. 3H). KCNK2, also known as TREK-1, has been reported in several studies to improve depressive disorders by blocking the TREK-1 tandem-pore potassium ion channel [34, 61, 62].

These results collectively demonstrate that through high throughput sequencing analysis and machine learning algorithms, we have identified TREK-1 as a key gene impacted by esketamine metabolites in improving postoperative depression.

Esketamine promotes the viability of hippocampal neurons by inhibiting TREK-1 two-pore domain potassium channels

To explore the effect of esketamine on the viability of rat hippocampal neurons under conditions of in vitro depression (CUMS), rat hippocampal neuron cell lines were initially isolated. Immunofluorescence was used to detect the proportions of neurons positive for the specific marker MAP2 and glial cells positive for the specific marker GFAP, showing a purity of neuronal cells exceeding 95%. The cells displayed good growth status, well-formed cell morphology, and clearly visible synaptic structures (Fig. 4A), indicating that the obtained neurons were suitable for subsequent experiments.

In order to simulate a depressive state in vitro, hippocampal neurons were pretreated with 300 μM NMDA for 24 h, followed by the introduction of 100 μg/ml esketamine to the treated cells. Consequently, the cells were divided into the control group, CUMS model group, CUMS + esketamine group, CUMS + esketamine + oe NC group, and CUMS + esketamine + oe TREK-1 group. Western blot experiments detected the expression of TREK-1 in the cell models. Compared to the control group, the expression of TREK-1 in the CUMS group significantly increased. In contrast, the TREK-1 expression in the CUMS + esketamine group was significantly decreased compared to the CUMS group, while in the CUMS + esketamine + oe TREK-1 group, the TREK-1 expression was significantly elevated compared to the CUMS + esketamine + oe NC group (Fig. 4B). These findings suggest that esketamine can influence the expression of TREK-1 in the rat hippocampal neuron model, with successful overexpression of TREK-1 achieved in the CUMS + esketamine + oe TREK-1 group.

Subsequently, the cell viability of primary hippocampal neurons in each group was assessed using the CCK-8 assay. The results indicated a significant

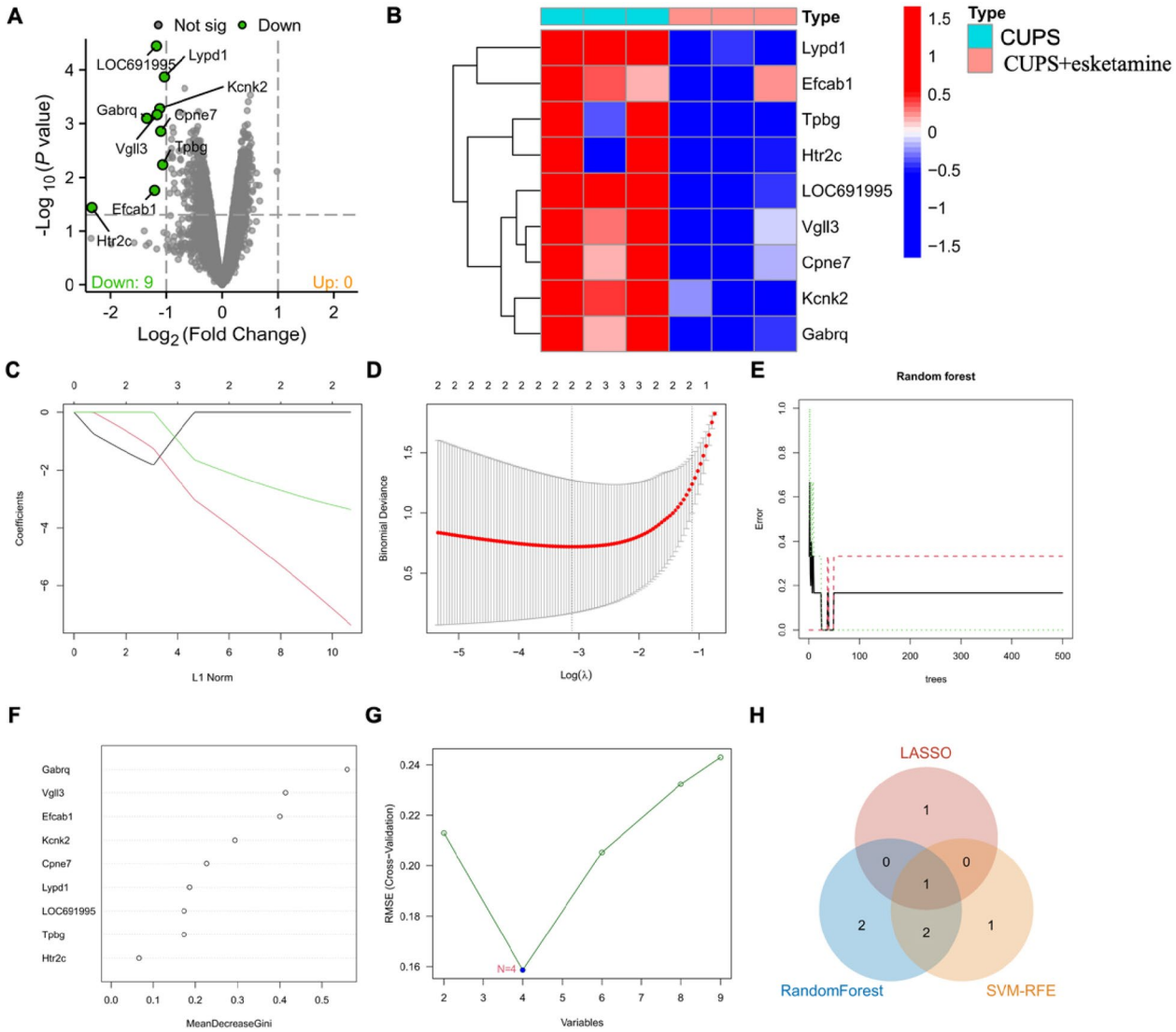

Fig. 3 Transcriptome sequencing analysis reveals the key role of TREK-1 in improving postoperative depression with esketamine metabolites. **A** Volcano plot of DEGs between 3 control (CUMS) and 3 esketamine treatment (CUMS + esketamine) groups of hippocampal neuron samples in high throughput sequencing data; **B** Heatmap revealing differential expression of 9 genes in the sequencing data; **C**, **D** LASSO coefficient selection plot; **E**, **F** Results plot of random forest algorithm; **G** SVM-RFE analysis results plot; **H** Venn diagram showing the intersection of genes related to the improvement of postoperative depression by esketamine metabolites selected by three machine learning algorithms: LASSO regression, random forest, and SVM-RFE

decrease in the viability of hippocampal neurons in the CUMS group compared to the control group. However, the CUMS + esketamine group exhibited a significant increase in cell viability compared to the CUMS group. Conversely, the CUMS + esketamine + oe TREK-1 group showed a significant decrease in hippocampal neuron cell viability compared to the CUMS + esketamine + oe NC group (Fig. 4C). Flow cytometry analysis revealed that the level of apoptosis in hippocampal neurons was significantly elevated in the CUMS group relative to the control group. In contrast, the CUMS + esketamine group demonstrated a significant reduction in apoptosis levels compared to the CUMS group. Furthermore, the level of apoptosis in hippocampal neurons was notably increased in the CUMS + esketamine + oe TREK-1 group compared to the CUMS + esketamine + oe NC group (Fig. 4D).

Using patch-clamp techniques, whole-cell potassium current changes in hippocampal neurons were examined. The results indicated a significant increase in potassium current levels in the CUMS group compared to the control group. In contrast, the CUMS + esketamine group displayed a significant decrease in potassium

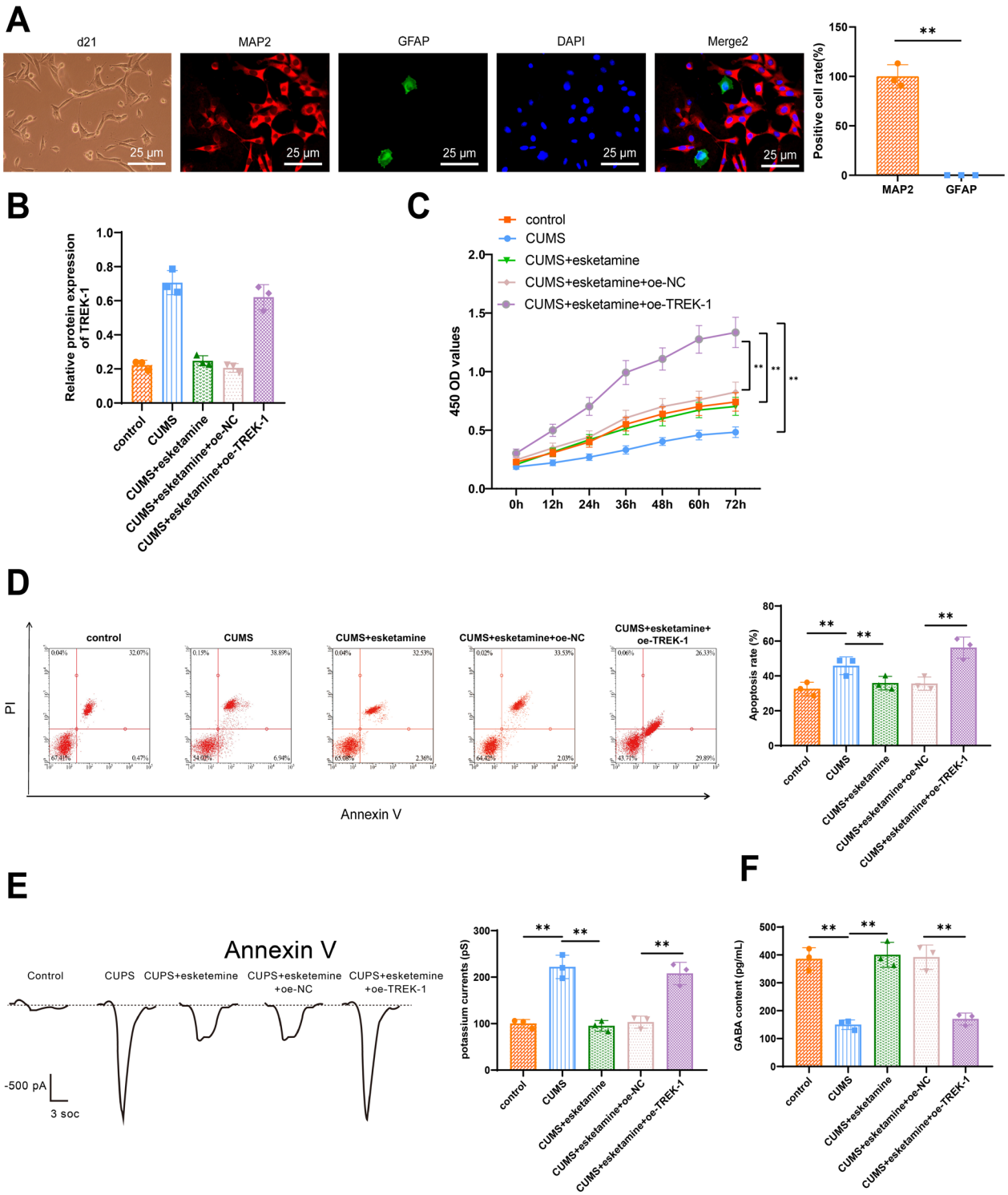

Fig. 4 Esketamine promotes hippocampal neuronal activity by inhibiting TREK-1 two-pore domain potassium channels. **A** Images of primary hippocampal neurons in rats, along with immunofluorescent identification of neuronal cells (MAP2, *red*) and glial cells (GFAP, *green*), with a scale bar of 20 μm; **B** Western blot analysis of TREK-1 protein expression in primary hippocampal neurons in rats after different treatments; **C** CCK-8 assay measuring changes in viability of primary hippocampal neurons in rats after different treatments; **D** Flow cytometry assessing the apoptosis rate of primary hippocampal neurons in rats after esketamine treatment; **E** Whole-cell patch clamp recording of potassium current levels in primary hippocampal neurons in rats after different treatments; **F** ELISA determining the neurotransmitter GABA content in primary hippocampal neurons in rats after different treatments. Cell experiments were repeated three times. $^{*}p < 0.05$, $^{**}p < 0.01$

current levels compared to the CUMS group. Similarly, the CUMS + esketamine + oe TREK-1 group exhibited a significant increase in potassium current levels compared to the CUMS + esketamine + oe NC group (Fig. 4E). Subsequent ELISA analysis of neurotransmitter levels in primary hippocampal neurons revealed that GABA protein levels were significantly reduced in the CUMS group compared to the control group. Conversely, the CUMS + esketamine group displayed a significant increase in GABA protein levels compared to the CUMS group. In contrast, the GABA protein levels in hippocampal neurons were notably decreased in the CUMS + esketamine + oe TREK-1 group compared to the CUMS + esketamine + oe NC group (Fig. 4F).

These outcomes suggest that esketamine may promote neuronal survival and functional improvement by inhibiting TREK-1 two-pore domain potassium channels, exerting a positive impact on the symptoms of postoperative depression in breast cancer.

Esketamine improves depressive symptoms in CUMS rats by inhibiting TREK-1 to enhance neuronal function

To corroborate the findings of in vitro experiments, we treated CUMS rats with esketamine, oe-TREK-1, and oe-NClentivirus, followed by a comprehensive evaluation of the animals. Results of the SPT indicated that compared to the Sham group, CUMS rats showed a significant decrease in sucrose intake. However, treatment with esketamine (10 mg/kg) led to a marked increase in sucrose consumption in CUMS rats compared to the CUMS group, while sucrose intake was significantly reduced in the CUMS + esketamine + oe TREK-1 group compared to the CUMS + esketamine + oe NC group (Fig. 5A). The FST results revealed that CUMS rats exhibited a

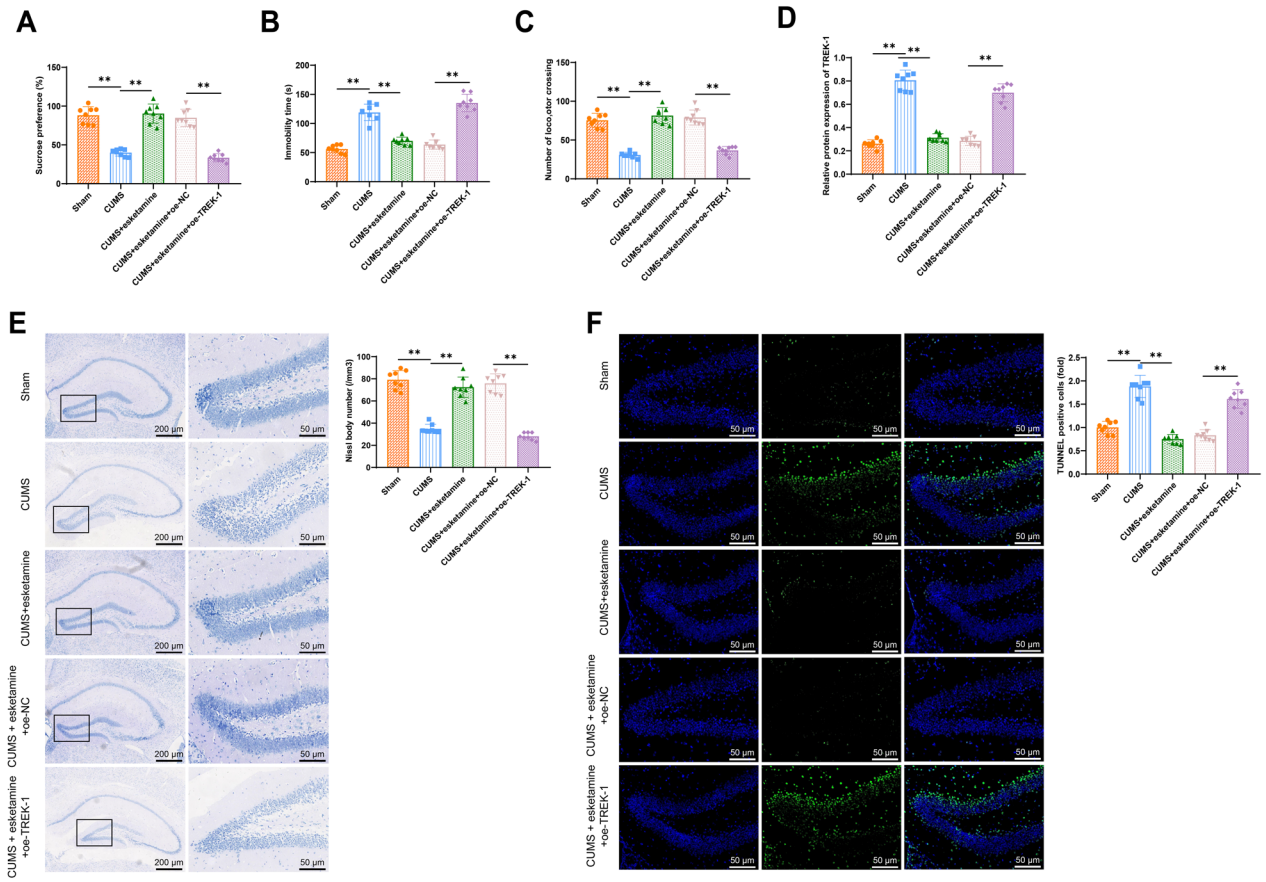

Fig. 5 Esketamine improves neuronal function and alleviates depressive symptoms in CUMS rats by inhibiting TREK-1. **A** Sucrose intake evaluation in CUMS depressive rat models after esketamine treatment combined with oe-NC and oe-TREK-1 ($n = 8$); **B** Statistical analysis of immobility time in CUMS depressive rat models after esketamine treatment combined with oe-NC and oe-TREK-1 ($n = 8$); **C** Statistical analysis of performance in OFT in CUMS depressive rat models after esketamine treatment combined with oe-NC and oe-TREK-1 ($n = 8$); **D** Western blot analysis of CUMS depressive rat models after esketamine treatment combined with oe-NC and oe-TREK-1 ($n = 8$); **E** Nissl staining to examine neuronal morphology, quantity, and distribution in the hippocampal region of CUMS depressive rat models after esketamine treatment combined with oe-NC and oe-TREK-1 ($n = 8$), with scale bars of 200 μm (*left*) and 50 μm (*right*); **F** TUNEL staining showing cell apoptosis in the hippocampal region of CUMS depressive rat models after esketamine treatment combined with oe-NC and oe-TREK-1 ($n = 8$), with a scale bar of 50 μm. $^{*}p < 0.05$, $^{**}p < 0.01$

significant increase in immobility time compared to the Sham group. Treatment with esketamine (10 mg/kg) significantly decreased immobility time in CUMS rats compared to the CUMS group. Notably, immobility time was significantly increased in the CUMS + esketamine + oe TREK-1 group compared to the CUMS + esketamine + oe NC group (Fig. 5B). Additionally, the OFT showed a significant decrease in the number of crossings by the CUMS group rats compared to the Sham group. Following treatment with esketamine (10 mg/kg), the number of crossings in the CUMS + esketamine group significantly increased compared to the CUMS group. Conversely, the CUMS + esketamine + oe TREK-1 group exhibited a significant decrease in the number of crossings compared to the CUMS + esketamine + oe NC group (Fig. 5C).

Subsequently, Western blot analysis was conducted to assess the expression levels of TREK-1 protein in the hippocampal region of rats under different treatment conditions. The results revealed a significant increase in TREK-1 protein expression in the hippocampal region of CUMS rats compared to the Sham group. However, in the CUMS + esketamine group, there was a significant decrease in TREK-1 protein expression compared to the CUMS group. Moreover, the CUMS + esketamine + oe TREK-1 group exhibited a significant increase in TREK-1 protein expression in the hippocampal region compared to the CUMS + esketamine + oe NC group (Fig. 5D).

Observations from Nissl staining demonstrated a significant decrease in the number of Nissl bodies in the hippocampal region of CUMS rats compared to the Sham group. Conversely, in the CUMS + esketamine group, there was a notable increase in the number of Nissl bodies in the CA1 pyramidal neurons of hippocampal region compared to the CUMS group. Furthermore, the CUMS + esketamine + oe TREK-1 group displayed a significant decrease in the number of Nissl bodies in the hippocampal region compared to the CUMS + esketamine + oe NC group (Fig. 5E).

Further investigation through TUNEL assay was carried out to examine cell apoptosis in the hippocampal region of rats. The results indicated a significant increase in cell apoptosis in the hippocampal region of CUMS rats compared to the Sham group. However, in the CUMS + esketamine group, there was a notable decrease in cell apoptosis in the hippocampal region compared to the CUMS group. Conversely, the CUMS + esketamine + oe TREK-1 group exhibited a significant increase in cell apoptosis in the hippocampal region compared to the CUMS + esketamine + oe NC group (Fig. 5F).

These findings suggest that esketamine can improve neuronal cell function and ultimately alleviate depressive symptoms in CUMS rats by inhibiting the activity of the TREK-1 protein.

Discussion

In this study, esketamine demonstrated significant antidepressant effects, consistent with its therapeutic effects on non-postoperative depression patients from other studies [63]. Unlike traditional selective serotonin reuptake inhibitors (SSRIs), esketamine acts rapidly, which is especially crucial for postoperative patients needing prompt symptom relief [64, 65]. While Esketamine's application in treating depression has been widely reported in the current literature, research on its specific use in post-breast cancer surgery patients remains limited [66]. This study addresses this gap by providing clinical evidence of esketamine's application in this patient population. In comparison to existing research, we delve more deeply into the drug's efficacy and its biological mechanisms [67, 68].

In studies on the neurobiological mechanisms of depression, TREK-1, a critical two-pore domain potassium channel, has been increasingly revealed to play a role in emotion regulation [61]. Previous research has predominantly focused on the basic biological characteristics of the TREK-1 channel. However, this study uniquely elucidates how esketamine improves symptoms of postoperative depression in breast cancer by regulating TREK-1. Through high throughput sequencing and machine learning techniques, this research not only confirms TREK-1's regulatory role in postoperative depression in breast cancer but also provides further insight into how esketamine executes its antidepressant effects by influencing this channel, a novel finding not previously reported in the literature.

Bioinformatics tools, particularly high throughput sequencing and machine learning algorithms played a crucial role in this study. These advanced techniques allowed for a comprehensive molecular-level understanding of esketamine's mechanism of action, a rarity in traditional antidepressant drug research. Compared to conventional biochemical analysis methods, the technical approach in this study enabled more precise gene and pathway identification, thereby enhancing the scientific rigor and reliability of the results. The application of this method not only optimized the screening process for candidate genes but also deepened our comprehension of the drug's mechanism of action.

The results of both in vitro cell experiments and in vivo animal model experiments in this study exhibited good consistency, reinforcing the hypothesis that esketamine improves depressive symptoms by modulating TREK-1. In the CUPS + esketamine + oe TREK-1 group, significant reductions in cell viability, crossings, and GABA levels, coupled with increased apoptosis, suggest that TREK-1 overexpression antagonizes the beneficial effects of esketamine. These results underscore the importance of

TREK-1 inhibition in the antidepressant mechanism of esketamine. TREK-1 overexpression may exacerbate neuronal dysfunction and disrupt neurotransmitter balance, emphasizing the necessity of targeted modulation rather than broad alteration of TREK-1 expression. These findings highlight the delicate balance in ion channel regulation required for therapeutic efficacy and the potential risks of unregulated TREK-1 activity.

The impact of esketamine on neurotransmitter release and cellular activity was significantly demonstrated in this study. In contrast to conventional antidepressants that primarily affect neurotransmitters such as serotonin or norepinephrine, esketamine improves neural function by directly targeting ion channels in nerve cells, shedding new light on the development of antidepressant medications [23, 69, 70]. Furthermore, this mechanism may explain why esketamine can rapidly alleviate depressive symptoms, providing a novel perspective for future antidepressant treatment strategies.

Considering the potential value of esketamine in the treatment of postoperative depression in breast cancer, its clinical application prospects are promising. The findings of this study support the possibility that esketamine can safely and effectively alleviate depressive symptoms in the short term, which is of significant importance for improving patients' immediate quality of life. However, further research is needed on the long-term safety and dosage adjustment of the drug to ensure its effectiveness and safety in broader clinical applications.

The present study systematically investigates the therapeutic potential of esketamine in alleviating symptoms of postoperative depression in breast cancer patients by modulating TREK-1 two-pore domain potassium channels, along with its underlying molecular genetic regulatory mechanisms. The results demonstrate that

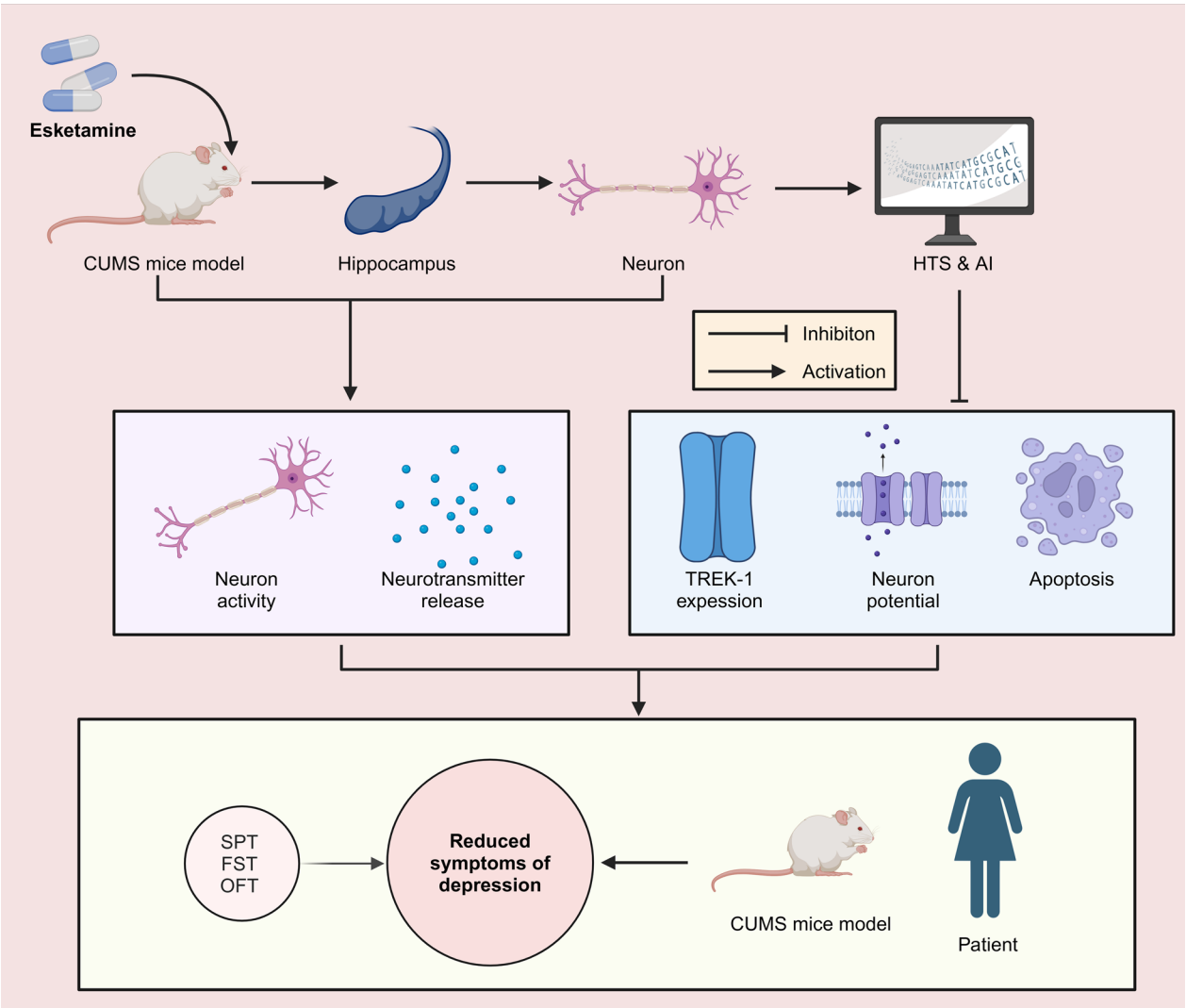

Fig. 6 Molecular mechanisms of esketamine in the treatment of postoperative depression in breast cancer

esketamine significantly inhibits the function of TREK-1 channels, thereby improving the functionality of hippocampal neuronal cells. Further experiments conducted in a rat model corroborate the potential efficacy of esketamine in alleviating depressive symptoms and its positive impact on neuronal survival and health (Fig. 6).

This research reveals the potential therapeutic role of esketamine in modulating TREK-1 two-pore domain potassium channels for postoperative depression in breast cancer patients, underscoring its significant scientific and clinical implications. Scientifically, this study not only advances our understanding of the biological mechanisms underlying depressive symptoms, particularly in the context of postoperative depression in breast cancer but also encourages further exploration of the role of TREK-1 channels in emotional regulation. Clinically, esketamine's rapid antidepressant effects offer a new treatment option for postoperative breast cancer patients who have not responded to traditional antidepressant therapies, promising to enhance their quality of life and overall well-being. Additionally, the discovery of this rapidly-acting antidepressant may steer future research and clinical practice toward more personalized and immediate strategies for treating depression.

Despite providing valuable insights into the treatment of postoperative depression in breast cancer, this study has several limitations. Firstly, the relatively small sample size may limit the generalizability and statistical power of the results. Secondly, the study primarily focuses on short-term observations of drug effects without assessing long-term therapeutic outcomes and safety. There were notable discrepancies between in vivo and in vitro results, such as more pronounced effects observed in animal models compared to in vitro experiments, likely due to the complex physiological environment in living organisms. Additionally, the effects of esketamine on key brain regions, such as the medial prefrontal cortex (mPFC), were not evaluated in in vitro assays, hindering a direct comparison of in vitro and in vivo findings. These limitations underscore the need for future studies to explore the drug's effects across different biological systems, conduct long-term evaluations, and validate findings through more extensive clinical trials involving a broader population to better understand the underlying biological mechanisms.

Based on the study results and identified limitations, future research should focus on several key areas. First, large-scale, multicenter clinical trials are necessary to validate the efficacy and safety of esketamine for treating postoperative depression in breast cancer patients, ensuring broader applicability of the findings. Additionally, it is crucial to explore the effects of esketamine across various depressive symptoms, particularly regarding long-term use, potential drug dependency, and side effects. In vitro studies should include detailed evaluations of esketamine's impact on specific brain regions, such as the medial prefrontal cortex and other hippocampal areas, to understand its precise neural mechanisms. While our findings suggest that TREK-1 modulation affects viability, apoptosis, and neurotransmitter levels, further research should investigate the specific biological pathways involving TREK-1 and its broader roles in the nervous system. These comprehensive studies aim to develop safer and more effective treatment strategies, ultimately providing substantial benefits to breast cancer patients suffering from postoperative depression.

Supplementary Information

The online version contains supplementary material available at https://doi.org/10.1186/s12935-025-03664-7.

Additional file 1: Figure S1. Enrichment analysis results of DEGs. Note: (A) Bar chart showing the GO enrichment of DEGs in high throughput sequencing results, where red, blue, and orange represent Biological Process (BP), Cellular Component (CC), and Molecular Function (MF) categories, respectively; (B) Bubble chart illustrating the KEGG enrichment of DEGs in high throughput sequencing results.

Additional file 2.

Acknowledgements
None.

Author contributions
Jiachi Xu and Hui Zhou conceived and designed the study. Yu Hu, Mingcan Li, and Qin Yang performed the experiments. Jiachi Xu and Hui Zhou analyzed the data. Jiachi Xu and Qin Yang wrote the manuscript. All authors reviewed and approved the final version of the manuscript.

Funding
Not applicable.

Data availability
No datasets were generated or analysed during the current study.

Declarations

Ethics approval and consent to participate
Clinical Trial was approved by Ethics Committee of The First Affiliated Hospital of University of South China (No. 20200304). All animal experiments were approved by the Animal Ethics Committee of The First Affiliated Hospital of University of South China (No.20200304).

Competing interests
The authors declare no competing interests.

Received: 15 July 2024 Accepted: 26 January 2025
Published online: 18 February 2025

References

1. Zhou X, Zhang X, Zhong T, Zhou M, Gao L, Chen L. Prevalence and associated factors of chemotherapy-related cognitive impairment in older

breast cancer survivors. J Adv Nurs. 2024;80(2):484–99. https://doi.org/10.1111/jan.15842.
2. Chang CY, Park H, Hincapie-Castillo JM, et al. Trends, characteristics, race, and ethnicity associated with nonadherence to antidepressants among breast cancer survivors with depression. J Manag Care Spec Pharm. 2023;29(4):431–45. https://doi.org/10.18553/jmcp.2023.29.4.431.
3. Suh LJ, Khan I, Kelley-Patteson C, Mohan G, Hassanein AH, Sinha M. Breast implant-associated immunological disorders. J Immunol Res. 2022;2022:8536149. https://doi.org/10.1155/2022/8536149.
4. Ugras SK, Layeequr RR. Hormone replacement therapy after breast cancer: yes, no or maybe? Mol Cell Endocrinol. 2021;525: 111180. https://doi.org/10.1016/j.mce.2021.111180.
5. Brown T, Cruickshank S, Noblet M. Specialist breast care nurses for support of women with breast cancer. Cochrane Database Syst Rev. 2021;2(2):CD005634. https://doi.org/10.1002/14651858.CD005634.pub3.
6. Dinapoli L, Colloca G, Di Capua B, Valentini V. Psychological aspects to consider in breast cancer diagnosis and treatment. Curr Oncol Rep. 2021;23(3):38. https://doi.org/10.1007/s11912-021-01049-3.
7. Zhu T, Goodarzi MO. Causes and consequences of polycystic ovary syndrome: insights from Mendelian randomization. J Clin Endocrinol Metab. 2022;107(3):e899–911. https://doi.org/10.1210/clinem/dgab757.
8. Singleton AC, Raeside R, Hyun KK, et al. Electronic health interventions for patients with breast cancer: systematic review and meta-analyses. J Clin Oncol. 2022;40(20):2257–70. https://doi.org/10.1200/JCO.21.01171.
9. Shammas RL, Marks CE, Broadwater G, et al. The effect of lavender oil on perioperative pain, anxiety, depression, and sleep after microvascular breast reconstruction: a prospective, single-blinded, randomized controlled trial. J Reconstr Microsurg. 2021;37(6):530–40. https://doi.org/10.1055/s-0041-1724465.
10. Chen W, Li J, Peng S, et al. Association of total thyroidectomy or thyroid lobectomy with the quality of life in patients with differentiated thyroid cancer with low to intermediate risk of recurrence. JAMA Surg. 2022;157(3):200–9. https://doi.org/10.1001/jamasurg.2021.6442.
11. Jordan RM, Oxenberg J. Breast Cancer Conservation Therapy. In: StatPearls. Treasure Island (FL): StatPearls Publishing; September 19, 2022.
12. Gassner L, Geretsegger M, Mayer-Ferbas J. Effectiveness of music therapy for autism spectrum disorder, dementia, depression, insomnia and schizophrenia: update of systematic reviews. Eur J Public Health. 2022;32(1):27–34. https://doi.org/10.1093/eurpub/ckab042.
13. Arnold I, Dehning J, Grunze A, Hausmann A. Old age bipolar disorder-epidemiology, aetiology and treatment. Medicina (Kaunas). 2021;57(6):587. https://doi.org/10.3390/medicina57060587.
14. Cipriani A. Carpe diem. Evid Based Ment Health. 2022;25(4):143–4. https://doi.org/10.1136/ebmental-2022-300608.
15. Goulart VG, Rocha-Mendonça H, Maisonnette S, Pandolfo P, Landeira-Fernandez J, Campello-Costa P. Differential expression of glutamatergic receptor subunits in the hippocampus in carioca high- and low-conditioned freezing rats. Mol Cell Neurosci. 2021;116: 103666. https://doi.org/10.1016/j.mcn.2021.103666.
16. Guo L, Gao T, Jia X, et al. SKF83959 attenuates memory impairment and depressive-like behavior during the latent period of epilepsy via allosteric activation of the sigma-1 receptor. ACS Chem Neurosci. 2022;13(22):3198–209. https://doi.org/10.1021/acschemneuro.2c00629.
17. Martins HC, Gilardi C, Sungur AÖ, et al. Bipolar-associated miR-499-5p controls neuroplasticity by downregulating the Cav1.2 subunit CACNB2. EMBO Rep. 2022;23(10):e54420. https://doi.org/10.15252/embr.202154420.
18. Mokhtar N, Doly S, Courteix C. Diabetic neuropathic pain and serotonin: what is new in the last 15 years? Biomedicines. 2023;11(7):1924. https://doi.org/10.3390/biomedicines11071924.
19. Bazovkina DV, Fursenko DV, Naumenko VS, Kulikov AV. The Role of C1473G polymorphism in mouse triptophan hydroxylase 2 gene in the acute effects of ethanol on the c-fos gene expression and metabolism of biogenic amines in the brain. Biochemistry (Mosc). 2023;88(3):291–302. https://doi.org/10.1134/S000629792303001X.
20. Huang Z, Liu N, Hu S, Ju X, Xu S, Wang S. Effect of Dexmedetomidine and two different doses of esketamine combined infusion on the quality of recovery in patients undergoing modified radical mastectomy for breast cancer - a randomised controlled study. Drug Des Devel Ther. 2023;17:2613–21. https://doi.org/10.2147/DDDT.S422896.
21. Wang M, Xiong HP, Sheng K, Sun XB, Zhao XQ, Liu QR. Perioperative administration of pregabalin and esketamine to prevent chronic pain after breast cancer surgery: a randomized controlled trial. Drug Des Devel Ther. 2023;17:1699–706. https://doi.org/10.2147/DDDT.S413273.
22. Shiiba S, Sago T, Kawabata K. Pain relief in short-lasting unilateral neuralgiform headache with conjunctival injection and tearing syndrome with intravenous ketamine: a case report. Acta Neurol Taiwan. 2021;30(1):35–8.
23. Hess EM, Riggs LM, Michaelides M, Gould TD. Mechanisms of ketamine and its metabolites as antidepressants. Biochem Pharmacol. 2022;197: 114892. https://doi.org/10.1016/j.bcp.2021.114892.
24. Jelen LA, Stone JM. Ketamine for depression. Int Rev Psychiatry. 2021;33(3):207–28. https://doi.org/10.1080/09540261.2020.1854194.
25. Johnston JN, Kadriu B, Kraus C, Henter ID, Zarate CA Jr. Ketamine in neuropsychiatric disorders: an update. Neuropsychopharmacology. 2024;49(1):23–40. https://doi.org/10.1038/s41386-023-01632-1.
26. Wei Q, Chen C, Zhu J, Mei B, Liu X. Influence of low-dose esketamine on postoperative depressive symptoms in patients with breast cancer (EASE): study protocol for a randomised controlled trial. BMJ Open. 2023;13(9): e075767. https://doi.org/10.1136/bmjopen-2023-075767.
27. Liu LL, Hu JH, Pan JJ, Liu H, Ji FH, Peng K. An intraoperative sub-anesthetic dose of esketamine on postoperative depressive symptoms in perimenopausal women with breast cancer undergoing modified radical mastectomy: protocol for a randomized, triple-blinded controlled trial. Int J Gen Med. 2023;16:3373–81. https://doi.org/10.2147/IJGM.S421265.
28. Ru Q, Lu Y, Saifullah AB, et al. TIAM1-mediated synaptic plasticity underlies comorbid depression-like and ketamine antidepressant-like actions in chronic pain. J Clin Invest. 2022;132(24): e158545. https://doi.org/10.1172/JCI158545.
29. Kim J, Kim TE, Lee SH, Koo JW. The role of glutamate underlying treatment-resistant depression. Clin Psychopharmacol Neurosci. 2023;21(3):429–46. https://doi.org/10.9758/cpn.22.1034.
30. Ren K, Liu H, Guo B, et al. Quercetin relieves D-amphetamine-induced manic-like behaviour through activating TREK-1 potassium channels in mice. Br J Pharmacol. 2021;178(18):3682–95. https://doi.org/10.1111/bph.15510.
31. Pope L, Minor DL Jr. The polysite pharmacology of TREK K^{2P} channels. Adv Exp Med Biol. 2021;1349:51–65. https://doi.org/10.1007/978-981-16-4254-8_4.
32. Lee EH, Park JE, Gotina L, et al. Novel potent blockers for TWIK-1/TREK-1 heterodimers as potential antidepressants. Biomed Pharmacother. 2023;165: 115139. https://doi.org/10.1016/j.biopha.2023.115139.
33. Walsh Y, Leach M, Veale EL, Mathie A. Block of TREK and TRESK K2P channels by lamotrigine and two derivatives sipatrigine and CEN-092. Biochem Biophys Rep. 2021;26: 101021. https://doi.org/10.1016/j.bbrep.2021.101021.
34. Cong T, Sun Y, Zhou Y, et al. Blocking two-pore domain potassium channel TREK-1 inhibits the activation of A1-like reactive astrocyte through the NF-κB signaling pathway in a rat model of major depressive disorder. Neurochem Res. 2023;48(6):1737–54. https://doi.org/10.1007/s11064-023-03857-4.
35. Kim SC, Kim A, Park JY, Hwang EM. Improved AAV vector system for cell-type-specific RNA interference. J Neurosci Methods. 2022;368: 109452. https://doi.org/10.1016/j.jneumeth.2021.109452.
36. Loo C, Glozier N, Barton D, et al. Efficacy and safety of a 4-week course of repeated subcutaneous ketamine injections for treatment-resistant depression (KADS study): randomised double-blind active-controlled trial. Br J Psychiatry. 2023;223(6):533–41. https://doi.org/10.1192/bjp.2023.79.
37. Boessen R, Groenwold RH, Knol MJ, Grobbee DE, Roes KC. Comparing HAMD(17) and HAMD subscales on their ability to differentiate active treatment from placebo in randomized controlled trials. J Affect Disord. 2013;145(3):363–9. https://doi.org/10.1016/j.jad.2012.08.026.
38. Liu P, Li P, Li Q, et al. Effect of pretreatment of s-ketamine on postoperative depression for breast cancer patients. J Invest Surg. 2021;34(8):883–8. https://doi.org/10.1080/08941939.2019.1710626.
39. Jiang N, Zhang BY, Dong LM, et al. Antidepressant effects of dammarane sapogenins in chronic unpredictable mild stress-induced depressive mice. Phytother Res. 2018;32(6):1023–9. https://doi.org/10.1002/ptr.6040.
40. Sang L, Kang K, Sun Y, Li Y, Chang B. FOXO4 ameliorates alcohol-induced chronic liver injury via inhibiting NF-κB and modulating gut microbiota in

C57BL/6J mice. Int Immunopharmacol. 2021;96: 107572. https://doi.org/10.1016/j.intimp.2021.107572.
41. Papp M, Gruca P, Lason-Tyburkiewicz M, Willner P. Antidepressant, anxiolytic and procognitive effects of subacute and chronic ketamine in the chronic mild stress model of depression. Behav Pharmacol. 2017;28(1):1–8. https://doi.org/10.1097/FBP.0000000000000259.
42. Li W, Liu D, Xu J, et al. Astrocyte-derived TNF-α-activated platelets promote cerebral ischemia/reperfusion injury by regulating the RIP1/RIP3/AKT signaling pathway. Mol Neurobiol. 2022;59(9):5734–49. https://doi.org/10.1007/s12035-022-02942-z.
43. Dai F, Wu J, Deng Z, et al. Integrated bioinformatic analysis of DNA methylation and immune infiltration in endometrial cancer. Biomed Res Int. 2022;2022:5119411. https://doi.org/10.1155/2022/5119411.
44. Liang X, Cheng Z, Chen X, Li J. Prognosis analysis of necroptosis-related genes in colorectal cancer based on bioinformatic analysis. Front Genet. 2022;13: 955424. https://doi.org/10.3389/fgene.2022.955424.
45. Du X, Qi H, Ji W, et al. Construction of a colorectal cancer prognostic risk model and screening of prognostic risk genes using machine-learning algorithms. Comput Math Methods Med. 2022;2022:9408839. https://doi.org/10.1155/2022/9408839.
46. Xin S, Liu X, Li Z, et al. ScRNA-seq revealed an immunosuppression state and tumor microenvironment heterogeneity related to lymph node metastasis in prostate cancer [published correction appears in Exp Hematol Oncol. 2024 May 20;13(1):54. https://doi.org/10.1186/s40164-024-00517-3]. Exp Hematol Oncol. 2023;12(1):49. Published 2023 May 23. https://doi.org/10.1186/s40164-023-00407-0
47. Chen K, Wang Y, Hou Y, et al. Single cell RNA-seq reveals the CCL5/SDC1 receptor-ligand interaction between T cells and tumor cells in pancreatic cancer. Cancer Lett. 2022;545: 215834. https://doi.org/10.1016/j.canlet.2022.215834.
48. Buchhalter JR, Dichter MA. Electrophysiological comparison of pyramidal and stellate nonpyramidal neurons in dissociated cell culture of rat hippocampus. Brain Res Bull. 1991;26(3):333–8. https://doi.org/10.1016/0361-9230(91)90003-3.
49. Zhang H, Zhou Z, Chen Z, Zhong Z, Li Z. Ginsenoside Rg3 exerts antidepressive effect on an NMDA-treated cell model and a chronic mild stress animal model. J Pharmacol Sci. 2017;134(1):45–54. https://doi.org/10.1016/j.jphs.2017.03.007.
50. Liu Z, Yu Y, Huang Z, et al. CircRNA-5692 inhibits the progression of hepatocellular carcinoma by sponging miR-328-5p to enhance DAB2IP expression. Cell Death Dis. 2019;10(12):900. https://doi.org/10.1038/s41419-019-2089-9.
51. Tang Y, Liu Y, Zhou H, et al. Esketamine is neuroprotective against traumatic brain injury through its modulation of autophagy and oxidative stress via AMPK/mTOR-dependent TFEB nuclear translocation. Exp Neurol. 2023;366: 114436. https://doi.org/10.1016/j.expneurol.2023.114436.
52. Cabanas H, Muraki K, Staines D, Marshall-Gradisnik S. Naltrexone restores impaired transient receptor potential melastatin 3 ion channel function in natural killer cells from myalgic encephalomyelitis/chronic fatigue syndrome patients. Front Immunol. 2019;10:2545. https://doi.org/10.3389/fimmu.2019.02545.
53. Salem M, Shan Y, Bernaudo S, Peng C. miR-590-3p targets cyclin G2 and FOXO3 to promote ovarian cancer cell proliferation, invasion, and spheroid formation. Int J Mol Sci. 2019;20(8):1810. https://doi.org/10.3390/ijms20081810.
54. Shu M, Zheng X, Wu S, et al. Targeting oncogenic miR-335 inhibits growth and invasion of malignant astrocytoma cells. Mol Cancer. 2011;10:59. https://doi.org/10.1186/1476-4598-10-59.
55. Jiang L, Zhou J, Zhao S, Wang X, Chen Y. STK17B promotes the progression of ovarian cancer. Ann Transl Med. 2021;9(6):475. https://doi.org/10.21037/atm-21-601.
56. Sun J, Li Y, Yang X, et al. Growth differentiation factor 11 accelerates liver senescence through the inhibition of autophagy. Aging Cell. 2022;21(1):e13532. https://doi.org/10.1111/acel.13532.
57. Wang YQ, Xu ZM, Wang XL, et al. LncRNA FOXC2-AS1 regulated proliferation and apoptosis of vascular smooth muscle cell through targeting miR-1253/FOXF1 axis in atherosclerosis. Eur Rev Med Pharmacol Sci. 2020;24(6):3302–14. https://doi.org/10.26355/eurrev_202003_20698.
58. Jiang D, Gong F, Ge X, et al. Neuron-derived exosomes-transmitted miR-124-3p protect traumatically injured spinal cord by suppressing the activation of neurotoxic microglia and astrocytes. J Nanobiotechnology. 2020;18(1):105. https://doi.org/10.1186/s12951-020-00665-8.
59. Wei CH, Wu G, Cai Q, et al. MicroRNA-330–3p promotes cell invasion and metastasis in non-small cell lung cancer through GRIA3 by activating MAPK/ERK signaling pathway [retracted in: J Hematol Oncol. 2020;13(1):142. https://doi.org/10.1186/s13045-020-00969-0]. J Hematol Oncol. 2017;10(1):125. https://doi.org/10.1186/s13045-017-0493-0
60. Venkatesan V, Madhira SL, Malakapalli VM, et al. Obesity, insulin resistance, and metabolic syndrome: a study in WNIN/Ob rats from a pancreatic perspective. Biomed Res Int. 2013;2013: 617569. https://doi.org/10.1155/2013/617569.
61. Francis-Oliveira J, Higa GSV, Viana FJC, et al. TREK-1 inhibition promotes synaptic plasticity in the prelimbic cortex. Exp Neurol. 2024;373: 114652. https://doi.org/10.1016/j.expneurol.2023.114652.
62. Xu H, Ding Y, Qi X, Zhang ZJ, Su J. Ameliorated neurogenesis deficits in dentate gyrus may underly the pronounced antidepressant effect of TREK-1 potassium channel blockade in rats with depressive-like behavior. ACS Chem Neurosci. 2022;13(21):3068–77. https://doi.org/10.1021/acschemneuro.2c00428.
63. Wang Y, He W, Zhang H, et al. mGluR5 mediates ketamine antidepressant response in susceptible rats exposed to prenatal stress. J Affect Disord. 2020;272:398–408. https://doi.org/10.1016/j.jad.2020.03.104.
64. Schoretsanitis G, Strømmen M, Krabseth HM, Helland A, Spigset O. Effects of sleeve gastrectomy and roux-en-Y gastric bypass on escitalopram pharmacokinetics: a cohort study. Ther Drug Monit. 2023;45(6):805–12. https://doi.org/10.1097/FTD.0000000000001114.
65. Kassie GM, Roughead EE, Nguyen TA, Pratt NL, Kalisch Ellett LM. The risk of preoperative central nervous system-acting medications on delirium following hip or knee surgery: a matched case-control study. Drug Saf. 2022;45(1):75–82. https://doi.org/10.1007/s40264-021-01136-1.
66. Kampling H, Baumeister H, Bengel J, Mittag O. Prevention of depression in adults with long-term physical conditions. Cochrane Database Syst Rev. 2021;3(3):CD011246. https://doi.org/10.1002/14651858.CD011246.pub2.
67. Schwenk ES, Pradhan B, Nalamasu R, et al. Ketamine in the Past, Present, and Future: Mechanisms, Metabolites, and Toxicity [published correction appears in Curr Pain Headache Rep. 2021 Sep 18;25(9):62. https://doi.org/10.1007/s11916-021-00985-w]. Curr Pain Headache Rep. 2021;25(9):57. https://doi.org/10.1007/s11916-021-00977-w
68. Meshkat S, Rodrigues NB, Di Vincenzo JD, et al. Pharmacogenomics of ketamine: a systematic review. J Psychiatr Res. 2021. https://doi.org/10.1016/j.jpsychires.2021.11.036.
69. Anand A, Mathew SJ, Sanacora G, et al. Ketamine versus ECT for nonpsychotic treatment-resistant major depression. N Engl J Med. 2023;388(25):2315–25. https://doi.org/10.1056/NEJMoa2302399.
70. McIntyre RS, Rosenblat JD, Nemeroff CB, et al. Synthesizing the evidence for ketamine and esketamine in treatment-resistant depression: an international expert opinion on the available evidence and implementation. Am J Psychiatry. 2021;178(5):383–99. https://doi.org/10.1176/appi.ajp.2020.20081251.

Publisher's Note